

# Supporting Information for "Elucidating the mechanisms responsible for Hadley cell weakening under $4 \times \text{CO}_2$ forcing"

R. Chemke <sup>1</sup>and L. M. Polvani <sup>2,3</sup>

<sup>1</sup>Department of Earth and Planetary Sciences, Weizmann Institute of Science, Rehovot, Israel

<sup>2</sup>Department of Applied Physics and Applied Mathematics, Columbia University, New York, NY, USA

<sup>3</sup>Department of Earth and Environmental Sciences, and Lamont-Doherty Earth Observatory, Columbia University, Palisades, NY,

USA

## Contents of this file

1. Table S1-S2

2. Figure S1-S3

---

**Table S1.** List of the 20 CMIP5 models analyzed in this study.

|    | <b>Model</b>  | <b>Modeling Center</b>  |
|----|---------------|---|
| 1  | ACCESS1.0     | CSIRO (Commonwealth Scientific and Industrial Research Organisation, Australia), and BOM (Bureau of Meteorology, Australia)   |
| 2  | BCC-CSM1-1    | Beijing Climate Center, China Meteorological Administration   |
| 3  | bcc-csm1-1-m  | Beijing Climate Center, China Meteorological Administration   |
| 4  | CanESM2       | Canadian Centre for Climate Modelling and Analysis  |
| 5  | CCSM4         | National Center for Atmospheric Research  |
| 6  | CNRM-CM5      | Centre National de Recherches Meteorologiques / Centre Europeen de Recherche et Formation Avancees en Calcul Scientifique   |
| 7  | CSIRO-Mk3-6-0 | Commonwealth Scientific and Industrial Research Organisation in collaboration with the Queensland Climate Change Centre of Excellence                                     |
| 8  | FGOALS-g2     | LASG, Institute of Atmospheric Physics, Chinese Academy of Sciences; and CESS, Tsinghua University  |
| 9  | GFDL-CM3      | Geophysical Fluid Dynamics Laboratory   |
| 10 | GFDL-ESM2G    | Geophysical Fluid Dynamics Laboratory   |
| 11 | GFDL-ESM2M    | Geophysical Fluid Dynamics Laboratory   |
| 12 | GISS-E2-H     | NASA Goddard Institute for Space Studies  |
| 13 | GISS-E2-R     | NASA Goddard Institute for Space Studies  |
| 14 | HadGEM2-ES    | Met Office Hadley Centre (additional HadGEM2-ES realizations contributed by Instituto Nacional de Pesquisas Espaciais)  |
| 15 | INMCM4        | Institute for Numerical Mathematics   |
| 16 | IPSL-CM5A-LR  | Institut Pierre-Simon Laplace   |
| 17 | IPSL-CM5B-LR  | Institut Pierre-Simon Laplace   |
| 18 | MIROC5        | Atmosphere and Ocean Research Institute (The University of Tokyo), National Institute for Environmental Studies, and Japan Agency for Marine-Earth Science and Technology |
| 19 | MRI-CGCM3     | Meteorological Research Institute   |
| 20 | NorESM1-M     | Norwegian Climate Centre  |

|                    | $\theta_y$ | $\theta_p$  | $OLR_y$ | $OLR - Q_{srf}$ | $OLR\theta_p^{-1}$ |
|--------------------|------------|-------------|---------|-----------------|--------------------|
| $Pq^{-1}$          | -0.03      | 0.53        | 0.01    | -0.04           | <b>0.61</b>        |
| $OLR\theta_p^{-1}$ | -0.11      | <b>0.92</b> | -0.17   | -0.22           |                    |
| $OLR - Q_{srf}$    | -0.05      | -0.27       | 0.16    |                 |                    |
| $OLR_y$            | -0.21      | -0.14       |         |                 |                    |
| $\theta_p$         | 0.13       |             |         |                 |                    |

**Table 2.** Cross-correlation of the quantities analyzed in this study. See Methods section in the main text for the definition of each quantity.

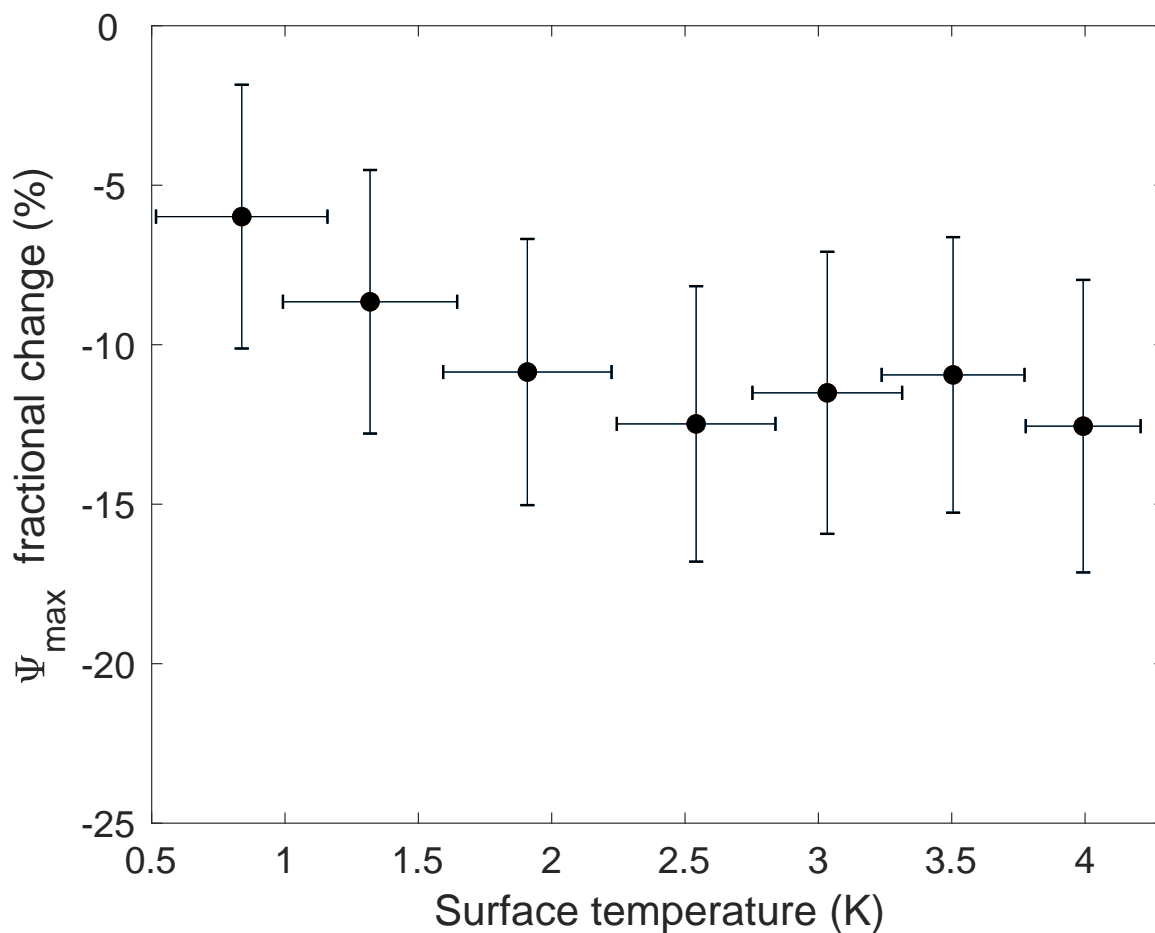


**Figure S1.** The fractional change (in %, relative to PI) in NH  $\Psi_{\max}$  under the abrupt  $4 \times \text{CO}_2$  forcing vs. the NH tropical mean surface temperature response (K). The error bars represent the 95% confidence interval calculated via Student's t-distribution across all models.

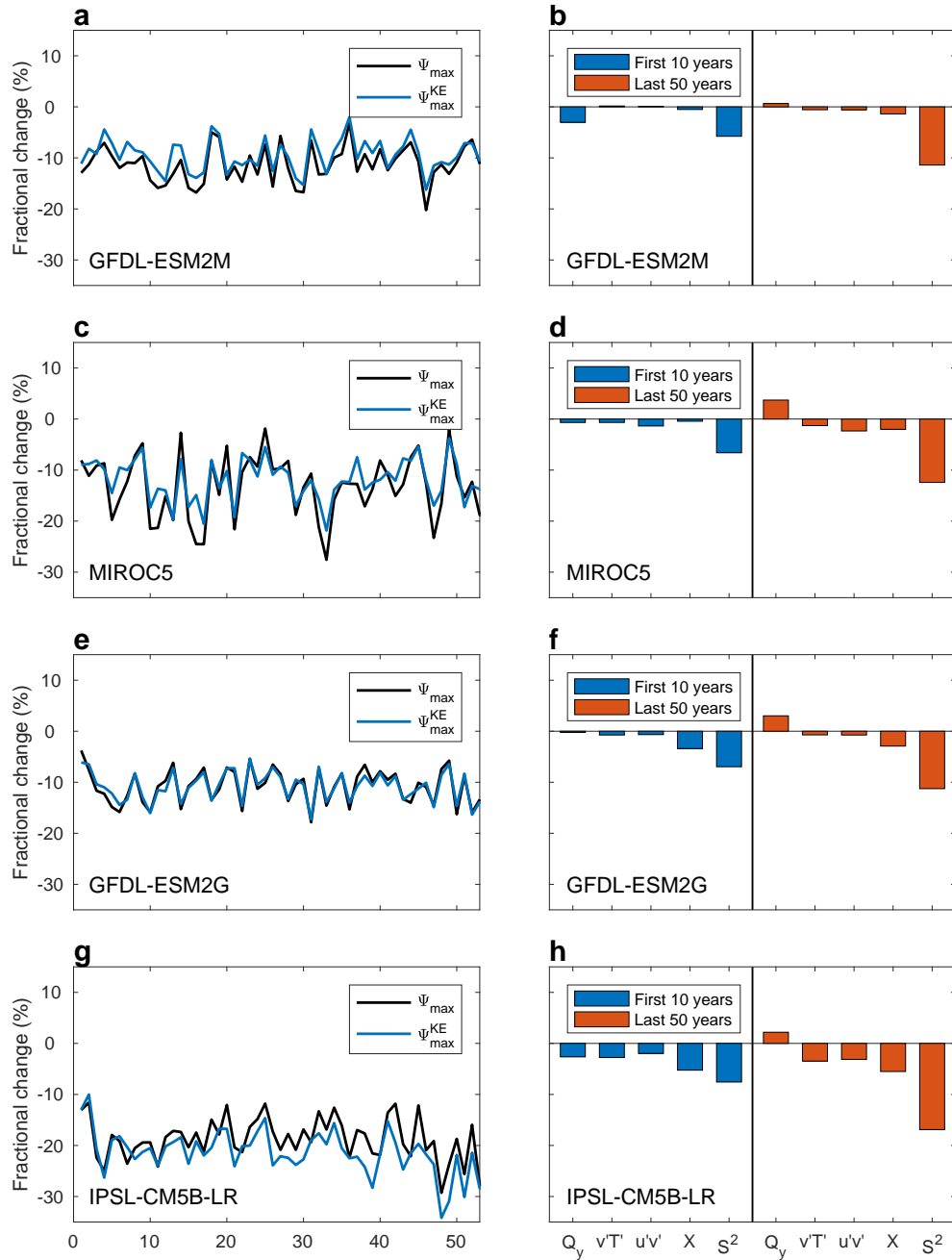


**Figure S2.** Time series of the fractional change (in %, relative to PI) of NH  $\Psi_{\max}$  (black line) and  $\Psi_{\max}^{\text{KE}}$  (blue line) under the abrupt  $4 \times \text{CO}_2$  forcing in CMIP5 (left column), and the relative contributions to changes in  $\Psi_{\max}^{\text{KE}}$  (right column) from: diabatic heating ( $Q_y$ ), eddy heat fluxes ( $v'T'$ ), eddy momentum fluxes ( $u'v'$ ), zonal friction ( $X$ ) and static stability ( $S^2$ ). The blue and red bars show the relative contributions to the first 10 years and last 50 years fractional change in  $\Psi_{\max}^{\text{KE}}$ , respectively. Each row shows the results from a different model.

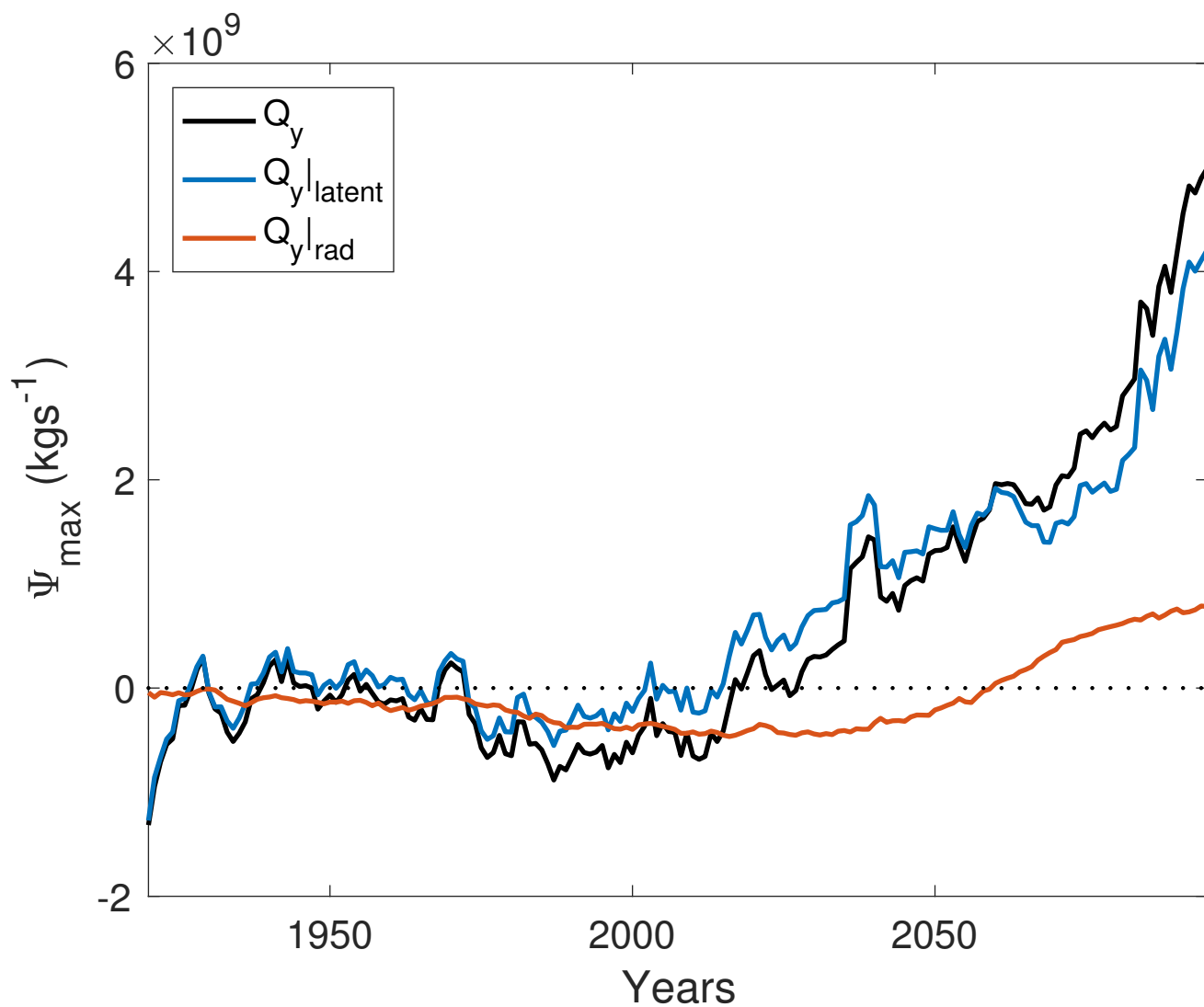


**Figure S3.** The relative contributions to changes in  $\Psi_{\max}^{\text{KE}}$  under the historical and RCP8.5 forcing in CESM LE from diabatic heating ( $Q_y$ , black), and from decomposing  $Q_y$  to latent ( $Q_y|_{\text{latent}}$ , blue) and radiative heating ( $Q_y|_{\text{rad}}$ , red)